Medicinal Chemistry Research (2019) 28:13–27
https://doi.org/10.1007/s00044-018-2258-x

MEDICINAL CHEMISTRY RESEARCH

ORIGINAL RESEARCH

Synthesis, antimalarial, antiproliferative, and apoptotic activities of benzimidazole-5-carboxamide derivatives

Jesús A. Romero[1] · María E. Acosta[1] · Neira D. Gamboa[1] · Michael R. Mijares[2,3] · Juan B. De Sanctis[2] · Ligia J. Llovera[4] · Jaime E. Charris[1]

Received: 3 July 2018 / Accepted: 2 November 2018 / Published online: 19 November 2018

Abstract

Twenty-eight compounds of the type N´-substituted-2-(5-nitroheterocyclic-2-yl)-3*H*-benzo[d]imidazole-5-carboxamide were obtained using as an oxidizing agent the nitrobenzene to obtain the benzimidazole scaffold, a modification of the Steglich esterification reaction was used to obtain the final compounds. The compounds were tested as potential inhibitors of the β-hematin formation in vitro, and in vivo were tested as antimalarial against mice infected by a strain of *Plasmodium berghei* ANKA sensitive to chloroquine. The survival time was increased by the compounds **3a** and **4d** to 17.00 ± 1.26 and 20.20 ± 1.95 days, while the progress of the infection was reduced to 4.02 ± 0.45 and 3.05 ± 0.09, respectively. The cytotoxic activity of all these compounds was assessed against Jurkat E6.1 and HL60 two human cancer cell line, and fresh human lymphocytes. Four compounds **4a**, **n** and **5a**, **n** showed enhanced cytotoxicity against Jurkat E6.1 and HL60 cell lines; fresh lymphocytes were not affected. Using flow cytometry, apoptotic cell death was observed at 24 h. The aforementioned compounds enhanced apoptosis both tumor cell lines decreasing cell survival by inhibiting autophagy.

Keywords Benzimidazol · Antimalarial · *P.berghei* · β-hematin · Antiproliferative · Apoptosis

Introduction

Malaria and cancer are two dissimilar illnesses that manifest themselves through different symptoms; however, they share similar metabolic requirements related to high proliferation rate (Njaria et al. 2015; Van Huijsduijnen et al. 2013). Countries in the tropics and subtropics are the most affected by malaria, which is transmitted by the bite of female Anopheles mosquitoes. There are five species that cause malaria in humans, namely *Plasmodium falciparum*, *vivax*, *ovale*, *malariae*, and lastly *knowlesi* (Singh et al. 2004). According to data reported in World Malaria Report, there were 216 million of new cases of malaria registered in 2016, up from 211 million cases in 2015, it was estimated that 445,000 people died due to complications of the disease in 2016. A similar number was reported for 2015, 446,000 (World Health Organization 2018a, 2018b) (WHO 2018a, 2018b). These numbers suggest that new treatments are needed.

Cancer is defined as a disease with an enhanced proliferative response and it is able to develop in any part of the body. It is considered the second leading cause of death worldwide, 8.8 million died from cancer in 2015. The most common cancer types are lung, gastric, liver, colon, breast, prostate, etc (WHO 2018a, 2018b).

Malaria can be prevented or treated through vector control with the use of residual insecticides or through chemotherapy. However, both the control of the vector and the treatment of the disease have been affected by the appearance of mosquitoes and strains of parasites resistant

Electronic supplementary material The online version of this article (https://doi.org/10.1007/s00044-018-2258-x) contains supplementary material, which is available to authorized users.

✉ Jaime E. Charris
jaime.charris@ucv.ve

[1] Laboratorio de Síntesis Orgánica, Unidad de Bioquímica, Facultad de Farmacia, Universidad Central de Venezuela, Apartado 47206, Los Chaguaramos, Caracas 1041, Venezuela

[2] Instituto de inmunología, Facultad de Medicina, Universidad Central de Venezuela, Apartado 50109, Caracas 1050, Venezuela

[3] Unidad de Biotecnología, Facultad de Farmacia, Universidad Central de Venezuela, Apartado 47206, Los Chaguaramos, Caracas 1041, Venezuela

[4] Laboratorio de Resonancia Magnética Nuclear, Centro de Química, Instituto Venezolano de Investigaciones Científicas, Altos de Pipe, Caracas 1020, Venezuela

to insecticides and chemotherapeutic agents of conventional use (US Centers for Disease Control and Prevention 2016) (CDC 2016; Noedl et al. 2008; Noedl et al. 2009; Dondorp et al. 2009). The RTS,S vaccine was rolled out in pilot tests involving three countries in sub-Saharan Africa (WHO 2018a, 2018b). Yet, an effective vaccine for malaria prophylaxis has not been developed to date (WHO 2016; Phillips et al. 2017).

Cancer can be treated by surgery, radiotherapy, and chemotherapy. However, side effects have always compromise patients' well being and enhanced comorbidities associated with the disease (Gupta et al. 2013). Moreover, several cancers are diagnosed and no other treatment besides chemotherapy can be provided to the patient.

Numerous studies have facilitated the identification of anticancer agents that have traditionally been employed in malaria chemotherapy, for example, chloroquine and its analogs (Rodrigues et al. 2012; Mushtaque 2015; Phillips et al. 2017; Romero et al. 2018; U.S. National Library of Medicine 2018). The mechanism through which chloroquine and its analogs exert their action could be related to inhibition of Bcl-2 protein family, increasing microautophagy in gliomas and inhibiting macroautophagy (Kim et al. 2010; Kundu et al. 2015; Nordstrøm et al. 2015). Also, an increase in the anticancer activity of chloroquine has been reported when it was administered in combination with anti-folate 5-FU, cisplatin, carboplatin agents, and sensitization of malignant cells to radiation (Kangwan et al. 2014). Artemisinins and its derivatives are also selectively cytotoxic to cancer cells in vitro, including drug- and radiation-resistant cancer cell lines (Efferth et al. 2003), in vivo in rodent models (Posner et al. 2004; Lai and Singh 2006), and have been used to treat human cancer patients (Berger et al. 2005; Singh and Panwar 2006; Efferth 2007).

Great efforts have been made with marginal results to determine the mechanism of action by which chloroquine and artemisinins eliminate the intra-erythrocytic forms of malaria parasite and enhance apoptosis in cancer cells. Both chloroquine and artemisinins have been proposed to inhibit a common target called hemozoin (Hz). Hz also known as malaria pigment, is a by-product formed by autoxidation of heme released during parasite digestion of host hemoglobin within the parasite food vacuole (Meshnick et al. 1991; Eganand Ncokazi 2005; Joshi and Viswanathan 2006; Zhang and Gerhard 2009; O'Neill et al. 2010; Zeng and Zhang 2011; Hooft van Huijsduijnen et al. 2013; Zhang et al. 2013). Artemisinins have been proposed to induce apoptosis through the intrinsic pathway involving Bcl-2, Bcl-XL, Bak/Bax, mitochondrial release of cytochrome c, loss of mitochondrial membrane potential, and activation of caspases 9 and 3 (Handrick et al.; 2010 Xu et al. 2011; Zhou et al. 2012). Thus, even though there are different pathways involved anti-malaria's can be efficient anti-tumor compounds.

Benzimidazole scaffold is present in numerous therapeutic agents such as antimicrobials, antiparasites, anticancer, antivirals, anti-inflammatory, antioxidants, proton pump inhibitors, antihypertensives, anticoagulants, immunomodulators, hormone modulators, CNS stimulants as well as depressants, lipid level modulators, antidiabetics, and other therapeutic agents has made it an indispensable anchor for development of new therapeutic agents (Camacho et al. 2011; Bansal and Silakari 2012; Gaba et al. 2014; Yadav and Ganguly 2015; Gaba and Mohan 2016; Akhtar et al. 2017; Lan et al. 2017). Another important group of compounds are those that contain nitroheterocyclic structures. These compounds are widely used in the treatment of protozoal and bacterial infections. Its mechanism of action seems to be related to the generation of free-radicals which in turn may have antitumuor, antiparasitic, and antibacterial agents (Cho et al. 2008; Brain-Isasi et al. 2008; Kim et al. 2009; Siriram et al. 2009; Mital 2009; Siriram et al. 2010; Hosseinzadeh et al. 2013). After extensive literature search, it has not been reported a combined structure with the aforementioned scaffolds. New structures may be more potent and selective as antimalarial and anticancer drugs.

Here, we report the synthesis of bezimidazole attached to a nitroheterocyclic structure which, in turn, was coupled, at position five, with a phenylcarboxamide substituted. The effect of the different compounds generated in two models: malaria infection, by *P. Berghei* in vitro and in vivo, and cytotoxic activities against tumor cell lines. A possible mechanism was proposed.

Material and methods

Chemical

All organic solvents (from Sigma-Aldrich Co. USA) were distilled and dried in the usual manner. A Thomas micro hot stage device was used to determine the melting points (mp) that were not corrected. A Nicolet^{TM} IS5 FT-IR (ID3 Zn-Se) spectrophotometer was used to determine the IR spectra. The ^{1}H NMR, ^{13}C NMR spectra were recorded using a Jeol Eclipse^{TM} 270 (270 MHz/67.9 MHz) spectrometer using Dimethyl Sulfoxide-d_6 ($DMSO_{d6}$) at ambient temperature, are reported in ppm downfield from the residual DMSO. The purity of the compounds was determined through the elemental analyses, using a Perkin Elmer 2400 CHN elemental analyzer, the results were within ± 0.4% of the predicted values. Compounds **3a** and **3b** were obtained previously (Charris et al. 2006).

General procedure for the synthesis of N ´-substituted-2-(5-nitrofuran or 5-nitrothiophe-2-yl)-3*H*-benzo[d]imidazole-5-carboxamide derivatives 4a–n, 5a–n

To **3a** and **3b** (0.3 mmol) in dry N,N-Dimethylformamide (DMF) 10 mL was added N-(3-Dimethylaminopropyl)-N ´-ethylcarbodiimide hydrochloride (EDC) (0.9 mmol), and 4-(Dimethylamino)-pyridine (DMAP) (0.4 mmol). The mixture was stirred at 0 °C for 1 h, the aniline respective (0.4 mmol) dissolved in dry DMF (2 mL) at 0 °C was added in a time of 30 min. The temperature of the mixture was carried to room temperature and stirred by 36 h, the thin layer chromatography (TLC) was used to monitor the progress of the reaction, and developed with cyclohexane:EtOAc:MeOH (7:2.5:0.5). An aqueous solution saturated with $NaHCO_3$ (20 mL) was used to quench the reaction. The solid resulting was filtered and slowly added water 5% KOH at 0 °C and the mixture stirred for 30 min. The solid was washed with water, methanol and ethyl ether, recrystallized from a mixture of ethanol and water (1:1) to give **4a–n**, **5a–n**.

N-(3,4,5-Trimethoxyphenyl)-2-(5-nitrofuran-2-yl)-1H-benzo [d]imidazole-5-carboxamide (4a)

Yield: 55%; mp: > 300 °C; IR (KBr pellet cm^{-1}): 1678 (C=O), 3500 (NH); ^{1}H NMR (DMSO-d_6): δ 3.65 (s, 3H, OCH_3), 3.79 (s, 6H, OCH_3), 7.27 (s, 2H, $H_{2",6"}$), 7.74 (d, 1H, $J = 8.6$ Hz, H_7), 7.89–7.92 (m, 2H, $H_{6,3'}$), 8.24 (d, 1H, $J = 4.4$ Hz, $H_{4'}$), 8.29 (s, 1H, H_4), 10.2 (s, 1H, NH). ^{13}C NMR (DMSO-d_6): δ 56.4, 60.7, 98.9, 123.7, 126.9, 130.5, 131.5, 134.5, 136.0, 140.9, 147.2, 150.8, 152.1, 153.2, 165.8. Anal. calcd. for $C_{21}H_{18}N_4O_7$: % C 57.53, H 4.14, N 12.78. Found % C 57.55, H 4.17, N, 12.91.

N-(2,4,-Dimethoxyphenyl)-2-(5-nitrofuran-2-yl)-1H-benzo[d] imidazole-5-carboxamide (4b)

Yield: 53%; mp: > 300 °C; IR (KBr pellet cm^{-1}): 1650 (C=O), 3572 (NH); ^{1}H NMR (DMSO-d_6): δ 3.70 (s, 3H, OCH_3), 3.77 (s, 3H, OCH_3), 6.71 (d, 1H, $J = 8.4$ Hz, $H_{6"}$), 7.01 (dd, 1H, $J = 8.4$, 1.5 Hz, $H_{5"}$), 7.62 (d, 1H, $J = 1.5$ Hz, $H_{3"}$), 7.74 (m, 2H, $H_{7,3'}$), 7.88 (d, 1H, J = 8.4 Hz, H_6), 8.24 (m, 2H, $H_{4',4}$), 10.20 (s, 1H, NH). ^{13}C NMR (DMSO-d_6): δ 56.1, 57.3, 109.4, 121.5, 127.1, 131.3, 131.7, 134.2, 136.3, 141.0, 147.6, 149.8, 151.7, 152.6, 166.1. Anal. calcd. for $C_{20}H_{16}N_4O_6$: % C 58.82, H 3.95, N 13.72. Found % C 58.87, H 4.01, N, 13.89.

N-(3-Methoxyphenyl)-2-(5-nitrofuran-2-yl)-1H-benzo[d] imidazole-5-carboxamide (4c)

Yield: 45%; mp: > 300 °C; IR (KBr pellet cm^{-1}): 1652 (C=O), 3578 (NH); ^{1}H NMR (DMSO-d_6): δ 3.76 (s, 3H, OCH_3), 6.67 (d, 1H, $J = 8.2$ Hz, $H_{4"}$), 7.25 (t, 1H, $J = 8.2$ Hz, $H_{5"}$), 7.40 (d, 1H, $J = 7.4$ Hz, $H_{6"}$), 7.51 (s, 1H, $H_{2"}$), 7.74 (d, 1H, $J = 8.2$ Hz, H_7), 7.89 (m, 2H, $H_{3',6}$), 8.24 (d, 1H, $J = 3.7$ Hz, $H_{4'}$), 8.28(s, 1H, H_4), 10.26 (s, 1H, NH). ^{13}C NMR (DMSO-d_6): δ 55.6, 106.7, 109.7, 113.2, 122.5, 123.9, 126.9, 129.9, 130.5, 131.5, 140.4, 141.1, 147.1, 152.1, 160.1, 166.2. Anal. calcd. for $C_{19}H_{14}N_4O_5$: % C 60.32, H 3.73, N 14.81. Found % C 60.32, H 3.75, N, 14.97.

N-(2,4-Dimethylphenyl)-2-(5-nitrofuran-2-yl)-1H-benzo[d] imidazole-5-carboxamide (4d)

Yield: 40%; mp: > 300 °C; IR (KBr pellet cm^{-1}): 1652 (C=O), 3570 (NH); ^{1}H NMR (DMSO-d_6): δ 2.2 (s, 3H, CH_3), 2.29 (s, 3H, CH_3), 7.02 (d, 1H, $J = 8.2$ Hz, $H_{5"}$), 7.08 (s, 1H, $H_{3"}$), 7.22 (d, 1H, $J = 8.1$ Hz, $H_{6"}$), 7.55 (d, 1H, $J =$ 4.0 Hz, $H_{3'}$), 7.73 (d, 1H, $J = 8.2$ Hz, H_7), 7.90 (m, 2H, $H_{6,4'}$), 8.28(s, 1H, H_4), 9.80 (s, 1H, NH). ^{13}C NMR (DMSO-d_6): δ 17.9, 20.7, 107.2, 109.9, 112.8, 120.8, 122.3, 125.6, 125.7, 128.4, 129.0, 133.7, 133.9, 134.1, 141.2, 147.3, 148.9, 165.8. Anal. calcd. for $C_{20}H_{16}N_4O_4$: % C 63.82, H 4.28, N 14.89. Found % C 63.84, H 4.30, N, 15.05.

N-(2,5-Dimethylphenyl)-2-(5-nitrofuran-2-yl)-1H-benzo[d] imidazole-5-carboxamide (4e)

Yield: 45%; mp: > 300 °C; IR (KBr pellet cm^{-1}): 1652 (C=O), 3570 (NH); ^{1}H NMR (DMSO-d_6): δ 2.23 (s, 3H, CH_3), 2.29 (s, 3H, CH_3), 7.05 (d, 1H, $J = 8.2$ Hz, $H_{4"}$), 7.08 (d, 1H, $J = 8.2$ Hz, $H_{3"}$), 7.20 (s, 1H, $H_{6"}$), 7.50 (d, 1H, $J =$ 4.0 Hz, $H_{3'}$), 7.71 (d, 1H, $J = 8.2$ Hz, H_7), 7.92 (m, 2H, $H_{6,4'}$), 8.29 (s, 1H, H_4), 10.02 (s, 1H, NH). ^{13}C NMR (DMSO-d_6): δ 18.1, 21.0, 106.9, 110.0, 112.3, 121.4, 121.9, 126.1, 126.9, 128.3, 129.7, 134.6, 135.1, 135.7, 139.8, 147.2, 148.0, 165.3. Anal. calcd. for $C_{20}H_{16}N_4O_4$: % C 63.82, H 4.28, N 14.89. Found % C 63.87, H 4.29, N, 15.17.

N-(3,4-Dimethylphenyl)-2-(5-nitrofuran-2-yl)-1H-benzo[d] imidazole-5-carboxamide (4f)

Yield: 53%; mp: > 300 °C; IR (KBr pellet cm^{-1}): 1650 (C=O), 3568 (NH); ^{1}H NMR (DMSO-d_6): δ 2.19 (s, 3H, CH_3), 2.22 (s, 3H, CH_3), 7.10 (d, 1H, $J = 7.9$ Hz, $H_{5"}$), 7.54 (m, 3H, $H_{2",3',6"}$), 7.73 (d, 1H, $J = 8.6$ Hz, H_7), 7.92 (m, 2H, $H_{6,4'}$), 8.27 (s, 1H, H_4), 10.15 (s, 1H, NH). ^{13}C NMR (DMSO-d_6): δ 18.9, 20.3, 100.9, 107.1, 109.8, 112.5, 121.1, 122.3, 125.3, 126.7, 128.1, 129.5, 134.3, 135.0, 136.1, 139.2, 147.1, 148.2, 165.7. Anal. calcd. for $C_{20}H_{16}N_4O_4$: % C 63.82, H 4.28, N 14.89. Found % C 63.82, H 4.31, N, 15.11.

N-(3,5-Dimethylphenyl)-2-(5-nitrofuran-2-yl)-1H-benzo[d] imidazole-5-carboxamide (4g)

Yield: 43%; mp: > 300 °C; IR (KBr pellet cm^{-1}): 1650 (C=O), 3565 (NH); ^{1}H NMR (DMSO-d_6): δ 2.28 (s, 6H, CH_3), 6.75 (s, 1H, $H_{4''}$), 7.44 (s, 2H, $H_{2'',6''}$), 7.56 (d, 1H, J = 3.5 Hz, $H_{3'}$), 7.73 (d, 1H, J = 8.4 Hz, H_7), 7.91 (m, 2H, $H_{6,4'}$), 8.28 (s, 1H, H_4), 10.12 (s, 1H, NH). ^{13}C NMR (DMSO-d_6): δ 21.8, 101.2, 106.4, 108.9, 113.0, 122.1, 122.6, 125.1, 127.0, 127.8, 129.3, 133.7, 135.2, 135.9, 139.1, 146.8, 147.0, 166.3. Anal. calcd. for $C_{20}H_{16}N_4O_4$: % C 63.82, H 4.28, N 14.89. Found % C 63.81, H 4.30, N, 15.07.

N-(3-Methylphenyl)-2-(5-nitrofuran-2-yl)-1H-benzo[d] imidazole-5-carboxamide (4h)

Yield: 39%; mp: > 300 °C; IR (KBr pellet cm^{-1}): 1652 (C=O), 3571 (NH); ^{1}H NMR (DMSO-d_6): δ 2.23 (s, 3H, CH_3), 7.10 (d, 1H, J = 8.2 Hz, $H_{4''}$), 7.50 (t, 1H, J = 7.2 Hz, $H_{5''}$), 7.58 (s, 1H, $H_{2''}$), 7.72 (d, 1H, J = 8.3 Hz, H_7), 7.90 (m, 3H, $H_{6,3',6''}$), 8.22 (d, 1H, J = 3.99 Hz, $H_{4'}$), 8.28 (s, 1H, H_4), 10.01 (s, 1H, NH). ^{13}C NMR (DMSO-d_6): δ 22.3, 99.8, 106.7, 107.3, 113.2, 121.7, 122.9, 124.7, 126.5, 127.7, 129.3, 134.7, 135.6, 138.7, 145.3, 147.4, 165.7. Anal. calcd. for $C_{19}H_{14}N_4O_4$: % C 62.98, H 3.89, N 15.46. Found % C 63.04, H 3.91, N, 15.71.

N-(2-Methylphenyl)-2-(5-nitrofuran-2-yl)-1H-benzo[d] imidazole-5-carboxamide (4i)

Yield: 49%; mp: > 300 °C; IR (KBr pellet cm^{-1}): 1659 (C=O), 3563 (NH); ^{1}H NMR (DMSO-d_6): δ 2.32 (s, 3H, CH_3), 6.91 (d, 1H, J = 8.2 Hz, $H_{3''}$), 7.23 (t, 1H, J = 7.9 Hz, $H_{4''}$), 7.59 (m, 3H, $H_{3',5'',6''}$), 7.73 (d, 1H, J = 8.9 Hz, H_7), 7.90 (m, 3H, $H_{6,4'}$), 8.29 (s, 1H, H_4), 10.19 (s, 1H, NH). ^{13}C NMR (DMSO-d_6): δ 21.7, 100.8, 107.1, 107.9, 113.9, 114.7, 117.9, 121.9, 124.8, 130.7, 134.5, 135.7, 137.8, 143.7, 147.7, 163.8. Anal. calcd. for $C_{19}H_{14}N_4O_4$: % C 62.98, H 3.89, N 15.46. Found % C 62.99, H 3.90, N, 15.65.

N-(3-Chloro-4-methoxyphenyl)-2-(5-nitrofuran-2-yl)-1H-benzo[d]imidazole-5-carboxamide (4j)

Yield: 37%; mp: > 300 °C; IR (KBr pellet cm^{-1}): 1650 (C=O), 3568 (NH); ^{1}H NMR (DMSO-d_6): δ 3.85 (s, 3H, OCH_3), 7.15 (d, 1H, J = 7.9 Hz, $H_{5''}$), 7.56 (m, 1H, $H_{2''}$), 7.72 (m, 1H, $H_{3',6''}$), 7.76 (d, 1H, J = 8.7 Hz, H_7), 7.91 (m, 2H, $H_{6,4'}$), 8.28 (s, 1H, H_4), 10.24 (s, 1H, NH). ^{13}C NMR (DMSO-d_6): δ 56.5, 101.2, 106.9, 113.7, 114.9, 117.0, 120.3, 121.9, 122.7, 123.4, 128.7, 133.1, 135.3, 136.7, 144.1, 147.1, 152.0, 165.7. Anal. calcd. for $C_{19}H_{13}ClN_4O_5$: % C 55.28, H 3.17, N 13.57. Found % C 55.28, H 3.19, N, 13.77.

N-(2-Chlorophenyl)-2-(5-nitrofuran-2-yl)-1H-benzo[d] imidazole-5-carboxamide (4k)

Yield: 32%; mp: > 300 °C; IR (KBr pellet cm^{-1}): 1652 (C=O), 3568 (NH); ^{1}H NMR (DMSO-d_6): δ 7.27 (d, 1H, J = 8.2 Hz, $H_{3''}$), 7.39 (t, 1H, J = 7.9 Hz, $H_{4''}$), 7.55 (d, 1H, J = 8.1 Hz, $H_{6''}$), 7.66 (t, 1H, J = 7.8 Hz, $H_{5''}$), 7.75 (d, 1H, J = 8.3 Hz, H_5), 7.93 (m, 2H, $H_{6,3'}$), 8.25 (m, 2H, $H_{4,4'}$), 10.02 (s, 1H, NH). ^{13}C NMR (DMSO-d_6): δ 102.1, 107.6, 113.0, 113.8, 115.8, 120.3, 122.7, 122.9, 123.9, 127.4, 128.7, 130.1, 133.1, 134.3, 136.5, 143.6, 145.4, 165.3. Anal. calcd. for $C_{18}H_{11}ClN_4O_4$: % C 56.48, H 2.90, N 14.64. Found % C 56.52, H 2.93, N, 14.90.

N-(4-Chlorophenyl)-2-(5-nitrofuran-2-yl)-1H-benzo[d] imidazole-5-carboxamide (4l)

Yield: 46%; mp: > 300 °C; IR (KBr pellet cm^{-1}): 1652 (C=O), 3568 (NH); ^{1}H NMR (DMSO-d_6): δ 7.41 (d, 2H, J = 9.1 Hz, $H_{3'',5''}$), 7.74 (d, 1H, J = 8.4 Hz, H_7), 7.84 (d, 2H, J = 9.1 Hz, $H_{2'',6''}$), 7.87 (d, 1H, J = 4.1 Hz, $H_{3'}$), 7.91 (m, 1H, H_6), 8.29 (m, 2H, $H_{4,4'}$), 10.32 (s, 1H, NH). ^{13}C NMR (DMSO-d_6): δ 102.3, 106.1, 112.9, 113.4, 115.2, 119.7, 122.4, 123.1, 123.7, 127.0, 128.5, 129.8, 133.4, 134.1, 136.7, 143.1, 145.2, 165.1. Anal. calcd. for $C_{18}H_{11}ClN_4O_4$: % C 56.48, H 2.90, N 14.64. Found % C 56.57, H 2.99, N, 14.98.

N-(4-Bromophenyl)-2-(5-nitrofuran-2-yl)-1H-benzo[d] imidazole-5-carboxamide (4m)

Yield: 38%; mp: > 300 °C; IR (KBr pellet cm^{-1}): 1656 (C=O), 3549 (NH); ^{1}H NMR (DMSO-d_6): δ 7.52 (d, 2H, J = 8.9 Hz, $H_{3'',5''}$), 7.77 (m, 3H, $H_{7,2'',6''}$), 7.92 (m, 2H, $H_{6,3'}$), 8.29 (m, 2H, $H_{4,4'}$), 10.37 (s, 1H, NH). ^{13}C NMR (DMSO-d_6): δ 102.7, 105.7, 115.4, 116.6, 118.9, 122.1, 123.6, 126.1, 128.4, 133.1, 139.3, 140.3, 153.2, 157.9, 165.7. Anal. calcd. for $C_{18}H_{11}BrN_4O_4$: % C 50.61, H 2.60, N 13.11. Found % C 50.69, H 2.56, N, 13.32.

N-[3-(Trifluoromethyl)phenyl]-2-(5-nitrofuran-2-yl)-1H-benzo[d]imidazole-5-carboxamide (4n)

Yield: 36%; mp: > 300 °C; IR (KBr pellet cm^{-1}): 1656 (C=O), 3543 (NH); ^{1}H NMR (DMSO-d_6): δ 7.44 (d, 1H, J = 7.9 Hz, $H_{4''}$), 7.61 (t, 1H, J = 7.4 Hz, $H_{5''}$), 7.76 (d, 1H, J = 8.2 Hz, H_7), 7.92 (m, 2H, $H_{3',2'',6''}$), 8.08 (d, 1H, J = 8.2 Hz, H_6), 8.24 (d, 1H, J = 3.9 Hz, $H_{4'}$), 10.55 (s, 1H, NH). ^{13}C NMR (DMSO-d_6): δ 101.5, 105.4, 115.4, 116.0, 117.3, 120.1, 122.8, 124.3, 124.9, 126.5, 129.3, 131.0, 136.4,

141.6, 152.7, 157.5, 159.1, 164.7. Anal. calcd. for $C_{19}H_{11}F_3N_4O_4$: % C 54.82, H 2.66, N 13.46. Found % C 54.85, H 2.72, N, 13.61.

N-(3,4,5-Trimethoxyphenyl)-2-(5-nitrothiophen-2-yl)-1H-benzo[d]imidazole-5-carboxamide (5a)

Yield: 52%; mp: > 300 °C; IR (KBr pellet cm^{-1}): 1680 (C=O), 3550 (NH); ^{1}H NMR (DMSO-d_6): δ 3.63 (s, 3H, OCH_3), 3.76 (s, 6H, OCH_3), 7.24 (s, 2H, $H_{2",6"}$), 7.70 (d, 1H, $J = 8.5$ Hz, H_7), 7.87 (m, 2H, $H_{6,3'}$), 8.23 (d, 1H, $J = 4.4$ Hz, $H_{4'}$), 8.26 (s, 1H, H_4), 10.12 (s, 1H, NH). ^{13}C NMR (DMSO-d_6): δ 56.4, 60.7, 98.9, 116.3, 123.9, 126.9, 130.6, 131.7, 134.4, 136.2, 140.4, 145.3, 147.2, 151.9, 153.2, 165.8. Anal. calcd. for $C_{21}H_{18}N_4O_6S$: % C 55.50, H 3.99, N 12.33. Found % C 55.61, H 4.09, N, 12.62.

N-(2,4,-Dimethoxyphenyl)-2-(5-nitrothiophen-2-yl)-1H-benzo[d]imidazole-5-carboxamide (5b)

Yield: 51%; mp: > 300 °C; IR (KBr pellet cm^{-1}): 1647 (C=O), 3577 (NH); ^{1}H NMR (DMSO-d_6): δ 3.67 (s, 3H, OCH_3), 3.75 (s, 3H, OCH_3), 6.77 (d, 1H, $J = 8.1$ Hz, $H_{6"}$), 7.10 (dd, 1H, $J = 8.4$, 1.8 Hz, $H_{5"}$), 7.69 (d, 1H, $J = 1.8$ Hz, $H_{3"}$), 7.74 (m, 2H, $H_{7,3'}$), 7.88 (d, 1H, $J = 8.4$ Hz, H_6), 8.23 (m, 2H, $H_{4',4}$), 9.29 (s, 1H, NH). ^{13}C NMR (DMSO-d_6): δ 56.1, 57.3, 99.8, 106.4, 115.9, 116.6, 121.5, 122.7, 123.6, 127.1, 131.0, 131.4, 140.0, 141.5, 142.3, 151.2, 152.9, 153.5, 156.7, 164.7. Anal. calcd. for $C_{20}H_{16}N_4O_5S$: % C 56.60, H 3.80, N 13.20. Found % C 56.63, H 3.82, N, 13.47.

N-(3-Methoxyphenyl)-2-(5-nitrothiophen-2-yl)-1H-benzo[d]imidazole-5-carboxamide (5c)

Yield: 51%; mp: > 300 °C; IR (KBr pellet cm^{-1}): 1648 (C=O), 3581 (NH); ^{1}H NMR (DMSO-d_6): δ 3.75 (s, 3H, OCH_3), 6.67 (d, 1H, $J = 6.7$ Hz, $H_{4"}$), 7.25 (t, 1H, $J = 7.7$ Hz, $H_{5"}$), 7.39 (d, 1H, $J = 7.7$Hz, $H_{6"}$), 7.56 (s, 1H, $H_{2"}$), 7.73 (d, 1H, $J = 8.4$ Hz, H_7), 7.89 (m, 2H, $H_{3',6}$), 8.17 (d, 1H, $J = 4.5$ Hz, $H_{4'}$), 8.29 (s, 1H, H_4), 10.25 (s, 1H, NH). ^{13}C NMR (DMSO-d_6): δ 55.6, 106.7, 109.7, 112.4, 115.3, 116.9, 122.9, 126.8, 129.9, 131.5, 140.7, 141.1, 150.5, 151.9, 158.9, 160.3, 166.1. Anal. calcd. for $C_{19}H_{14}N_4O_4S$: % C 57.86, H 3.58, N 14.21. Found % C 57.89, H 3.61, N, 14.38.

N-(2,4-Dimethylphenyl)-2-(5-nitrothiophen-2-yl)-1H-benzo[d]imidazole-5-carboxamide (5d)

Yield: 48%; mp: > 300 °C; IR (KBr pellet cm^{-1}): 1651 (C=O), 3577 (NH); ^{1}H NMR (DMSO-d_6): δ 2.25 (s, 3H, CH_3), 2.28 (s, 3H, CH_3), 7.09 (d, 1H, $J = 8.7$ Hz, $H_{5"}$), 7.13 (s, 1H, $H_{3"}$), 7.21 (d, 1H, $J = 8.6$ Hz, $H_{6"}$), 7.60 (d, 1H, $J = 3.9$ Hz, $H_{3'}$), 7.72 (d, 1H, $J = 8.2$ Hz, H_7), 7.92 (m, 2H, $H_{6,4'}$), 8.25(s, 1H, H_4), 9.79 (s, 1H, NH). ^{13}C NMR (DMSO-d_6): δ 17.5, 21.9, 112.8, 116.1, 120.8, 122.1, 126.0, 128.4, 129.2, 130.7, 131.3, 132.2, 133.9, 134.1, 140.1, 141.3, 142.2, 151.3, 152.9, 164.8. Anal. calcd. for $C_{20}H_{16}N_4O_3S$: % C 61.21, H 4.11, N 14.28. Found % C 61.27, H 4.17, N, 14.61.

N-(2,5-Dimethylphenyl)-2-(5-nitrothiophen-2-yl)-1H-benzo[d]imidazole-5-carboxamide (5e)

Yield: 49%; mp: > 300 °C; IR (KBr pellet cm^{-1}): 1659 (C=O), 3561 (NH); ^{1}H NMR (DMSO-d_6): δ 2.26 (s, 3H, CH_3), 2.27 (s, 3H, CH_3), 7.02 (d, 1H, $J = 8.1$ Hz, $H_{4"}$), 7.07 (d, 1H, $J = 8.2$ Hz, $H_{3"}$), 7.27 (s, 1H, $H_{6"}$), 7.55 (d, 1H, $J = 4.0$ Hz, $H_{3'}$), 7.73 (d, 1H, $J = 8.2$ Hz, H_7), 7.89 (m, 2H, $H_{6,4'}$), 8.30(s, 1H, H_4), 10.10 (s, 1H, NH). ^{13}C NMR (DMSO-d_6): δ 18.1, 22.7, 106.9, 112.3, 121.7, 122.9, 124.5, 126.9, 128.7, 129.7, 131.6, 135.1, 135.7, 139.8, 145.1, 148.0, 150.9, 151.3, 164.3. Anal. calcd. for $C_{20}H_{16}N_4O_3S$: % C 61.21, H 4.11, N 14.28. Found % C 61.23, H 4.15, N, 14.43.

N-(3,4-Dimethylphenyl)-2-(5-nitrothiophen-2-yl)-1H-benzo[d]imidazole-5-carboxamide (5f)

Yield: 45%; mp: > 300 °C; IR (KBr pellet cm^{-1}): 1648 (C=O), 3570 (NH); ^{1}H NMR (DMSO-d_6): δ 2.17 (s, 3H, CH_3), 2.23 (s, 3H, CH_3), 7.09 (d, 1H, $J = 8.3$ Hz, $H_{5"}$), 7.52 (m, 3H, $H_{2",3',6"}$), 7.76 (d, 1H, $J = 8.3$ Hz, H_7), 7.91 (m, 2H, $H_{6,4'}$), 8.25 (s, 1H, H_4), 10.17 (s, 1H, NH). ^{13}C NMR (DMSO-d_6): δ 18.9, 19.7, 99.9, 109.6, 112.5, 118.3, 121.1, 122.5, 125.3, 126.4, 128.3, 129.4, 134.1, 134.9, 139.6, 146.9, 147.8, 149.9, 151.1, 165.3. Anal. calcd. for $C_{20}H_{16}N_4O_3S$: % C 61.21, H 4.11, N 14.28. Found % C 61.32, H 4.20, N, 14.52.

N-(3,5-Dimethylphenyl)-2-(5-nitrothiophen-2-yl)-1H-benzo[d]imidazole-5-carboxamide (5g)

Yield: 51%; mp: > 300 °C; IR (KBr pellet cm^{-1}): 1652 (C=O), 3568 (NH); ^{1}H NMR (DMSO-d_6): δ 2.27 (s, 6H, CH_3), 6.74 (s, 1H, $H_{4"}$), 7.44 (s, 2H, $H_{2",6"}$), 7.57 (d, 1H, $J = 4.1$ Hz, $H_{3'}$), 7.69 (d, 1H, $J = 8.2$ Hz, H_7), 7.97 (m, 2H, $H_{6,4'}$), 8.32 (s, 1H, H_4), 10.15 (s, 1H, NH). ^{13}C NMR (DMSO-d_6): δ 22.6, 101.4, 106.4, 118.9, 122.6, 127.3, 128.8, 130.3, 136.5, 137.4, 139.1, 145.4, 147.6, 150.9, 151, 7, 163.9. Anal. calcd. for $C_{20}H_{16}N_4O_3S$: % C 61.21, H 4.11, N 14.28. Found % C 61.29, H 4.19, N, 14.48.

N-(3-Methylphenyl)-2-(5-nitrothiophen-2-yl)-1H-benzo[d] imidazole-5-carboxamide (5h)

Yield: 37%; mp: > 300 °C; IR (KBr pellet cm^{-1}): 1650 (C=O), 3565 (NH); ^{1}H NMR (DMSO-d_6): δ 2.24 (s, 3H, CH_3), 7.14 (d, 1H, J = 8.6 Hz, $H_{4''}$), 7.53 (t, 1H, J = 7.2 Hz, $H_{5''}$), 7.61 (s, 1H, $H_{2''}$), 7.75 (d, 1H, J = 8.7 Hz, H_7), 7.92 (m, 3H, $H_{6,3',6''}$), 8.25 (d, 1H, J = 4.04 Hz, $H_{4'}$), 8.31 (s, 1H, H_4), 10.07 (s, 1H, NH). ^{13}C NMR (DMSO-d_6): δ 22.3, 100.8, 106.7, 113.2, 121.7, 124.9, 125.7, 126.5, 129.3, 134.7, 135.6, 138.6, 139.0, 145.3, 147.2, 151.0, 153.1, 164.7. Anal. calcd. for $C_{19}H_{14}N_4O_3S$: % C 60.31, H 3.73, N 14.81. Found % C 60.31, H 3.75, N, 14.97.

N-(2-Methylphenyl)-2-(5-nitrothiophen-2-yl)-1H-benzo[d] imidazole-5-carboxamide (5i)

Yield: 45%; mp: > 300 °C; IR (KBr pellet cm^{-1}): 1658 (C=O), 3562 (NH); ^{1}H NMR (DMSO-d_6): δ 2.28 (s, 3H, CH_3), 6.92 (m, 1H, $H_{3''}$), 7.15 (t, 1H, J = 7.7 Hz, $H_{4''}$), 7.69 (m, 4H, $H_{5,3',5'',6''}$), 7.94 (m, 3H, $H_{6,4'}$), 8.23 (s, 1H, H_4), 10.12 (s, 1H, NH). ^{13}C NMR (DMSO-d_6): δ 18.7, 100.8, 107.1, 117.9, 121.8, 124.3, 127.0, 127.9, 130.7, 134.5, 135.7, 139.8, 143.7, 147.7, 150.6, 152.4, 164.7. Anal. calcd. for $C_{19}H_{14}N_4O_3S$: % C 60.31, H 3.73, N 14.81. Found % C 60.40, H 3.76, N, 15.03.

N-(3-Chloro-4-methoxyphenyl)-2-(5-nitrothiophen-2-yl)-1H-benzo[d]imidazole-5-carboxamide (5j)

Yield: 46%; mp: > 300 °C; IR (KBr pellet cm^{-1}): 1656 (C=O), 3565 (NH); ^{1}H NMR (DMSO-d_6): δ 3.84 (s, 3H, OCH_3), 7.18 (d, 1H, J = 7.9 Hz, $H_{5''}$), 7.55 (m, 1H, $H_{2''}$), 7.74 (m, 1H, $H_{3',6''}$), 7.79 (d, 1H, J = 8.9 Hz, H_7), 7.92 (m, 2H, $H_{6,4'}$), 8.29 (s, 1H, H_4), 10.21 (s, 1H, NH). ^{13}C NMR (DMSO-d_6): δ 55.4, 101.2, 106.9, 114.7, 115.9, 117.3, 120.1, 121.8, 122.8, 123.4, 129.7, 133.0, 133.3, 139.7, 143.8, 144.1, 150.1, 152.9, 164.7. Anal. calcd. for $C_{19}H_{13}ClN_4O_4S$: % C 53.21, H 3.06, N 13.06. Found % C 53.25, H 3.11, N, 13.31.

N-(2-Chlorophenyl)-2-(5-nitrothiophen-2-yl)-1H-benzo[d] imidazole-5-carboxamide (5k)

Yield: 37%; mp: > 300 °C; IR (KBr pellet cm^{-1}): 1658 (C=O), 3567 (NH); ^{1}H NMR (DMSO-d_6): δ 7.28 (d, 1H, J = 8.5 Hz, $H_{3''}$), 7.37 (t, 1H, J = 7.8 Hz, $H_{4''}$), 7.65 (m, 2H, J = 8.1 Hz, $H_{5'',6''}$), 7.73 (d, 1H, J = 8.9 Hz, H_5), 7.92 (m, 1H, H_6), 8.24 (m, 1H, $H_{4'}$), 8.30 (s, 1H, H_4), 10.13 (s, 1H, NH). ^{13}C NMR (DMSO-d_6): δ 102.1, 107.6, 120.3, 122.7, 122.9, 125.9, 127.2, 127.4, 128.7, 129.1, 130.2, 133.5, 134.9, 136.5, 143.6, 145.4, 151.2, 152.4, 165.8. Anal. calcd. for $C_{18}H_{11}ClN_4O_3S$: % C 54.21, H 2.78, N 14.05. Found % C 54.22, H 2.81, N, 13.90.

N-(4-Chlorophenyl)-2-(5-nitrothiophen-2-yl)-1H-benzo[d] imidazole-5-carboxamide (5l)

Yield: 39%; mp: > 300 °C; IR (KBr pellet cm^{-1}): 1652 (C=O), 3573 (NH); ^{1}H NMR (DMSO-d_6): δ 7.40 (d, 2H, J = 8.4 Hz, $H_{3'',5''}$), 7.71 (d, 1H, J = 8.4 Hz, H_7), 7.84 (m, 4H, $H_{6',3',2'',6''}$), 8.23 (d, 1H, J = 4.2 Hz, $H_{4'}$), 10.41 (s, 1H, NH). ^{13}C NMR (DMSO-d_6): δ 101.3, 106.1, 122.4, 123.4, 123.7, 127.4, 129.5, 133.4, 134.1, 138.7, 143.1, 145.2, 151.1, 153.0, 165.1. Anal. calcd. for $C_{18}H_{11}ClN_4O_3S$: % C 54.21, H 2.78, N 14.05. Found % C 54.27, H 2.83, N, 14.29.

N-(4-Bromophenyl)-2-(5-nitrothiophen-2-yl)-1H-benzo[d] imidazole-5-carboxamide (5m)

Yield: 35%; mp: > 300 °C; IR (KBr pellet cm^{-1}): 1660 (C=O), 3565 (NH); ^{1}H NMR (DMSO-d_6): δ 7.53 (d, 2H, J = 8.5 Hz, $H_{3'',5''}$), 7.73 (d, 1H, J = 8.1 Hz, H_7), 7.80 (d, 2H, J = 8.5 Hz, $H_{2'',6''}$), 7.89 (m, 2H, $H_{6,3'}$), 8.23 (d, 1H, J = 4.4 Hz, $H_{4'}$), 8.29 (s, 1H, H_4), 10.32 (s, 1H, NH). ^{13}C NMR (DMSO-d_6): δ 101.7, 107.7, 118.4, 122.1, 123.5, 126.1, 128.1, 129.3, 133.0, 139.1, 141.7, 142.4, 150.1, 152.9, 165.5. Anal. calcd. for $C_{18}H_{11}BrN_4O_3S$: % C 48.77, H 2.50, N 12.64. Found % C 48.81, H 2.54, N, 12.90.

N-[3-(Trifluoromethyl)phenyl]-2-(5-nitrothiophen-2-yl)-1H-benzo[d]imidazole-5-carboxamide (5n)

Yield: 36%; mp: > 300 °C; IR (KBr pellet cm^{-1}): 1656 (C=O), 3549 (NH); ^{1}H NMR (DMSO-d_6): δ 7.40 (d, 1H, J = 7.4 Hz, $H_{4''}$), 7.59 (t, 1H, J = 7.7 Hz, $H_{5''}$), 7.67 (d, 1H, J = 8.4 Hz, H_7), 7.93 (m, 3H, $H_{3',2'',6''}$), 8.07 (d, 1H, J = 8.4 Hz, H_6), 8.27 (d, 1H, J = 3.9 Hz, $H_{4'}$), 8.32 (s, 1H, H_4), 10.56 (s, 1H, NH). ^{13}C NMR (DMSO-d_6): δ 101.5, 105.4, 117.9, 121.8, 122.1, 122.8, 123.9, 124.7, 126.3, 129.1, 130.2, 131.0, 133.1, 138.4, 141.7, 142.4, 150.7, 152.5, 164.1. Anal. calcd. for $C_{19}H_{11}F_3N_4O_3S$: % C 52.78, H 2.56, N 12.96. Found % C 52.83, H 2.59, N, 13.21.

Biological assays

Inhibition of β-hematin formation

The β-hematin (β-H) (synthetic haemozoin) formation assay was assessed according previously described protocol (Baelmans et al. 2000). A hemin chloride solution (50 µL, 4 mM), was made in DMSO (5.2 mg mL^{-1}). Then, it was distributed in 96-well micro plates. The compounds were dissolved in DMSO and different concentrations (100-5

mM) were added in test wells (50 µL). The experiments were performed in triplicate. Water (50 µL) or DMSO (50 µL) were used as controls. Acetate buffer (100 µL 0.2 M, pH 4.4) was used to generate β-H. Then, the plates were incubated at 37 °C for 48 h and centrifuged (4000 RPMx15 min, IEC-CENTRA, MP4R). The supernatant was discarded, and the pellet was washed twice with DMSO (200µL) and dissolved in NaOH (200µL, 0.2 N). The aggregates were further solubilized with NaOH (0.1 N) and absorbances recorded at 405 nm (Microplate Reader, BIORAD-550). The results were expressed as a percentage of β-H (synthetic haemozoin) formation inhibition (Charris et al. 2007; Romero et al. 2018).

Parasite, experimental host, and strain maintenance

Male Balb-C mice, weighing 18–22 g were maintained on a commercial pellet diet ad libitum and under conditions approved by Ethics Committee of the Institute of Immunology. A rodent malaria ANKA strain of *Plasmodium berghei*, parasite, was used to infect the animals. Infected erythrocytes, 1×10^6 erythrocytes diluted in phosphate buffered saline solution (PBS, 10 mM, pH 7.4, 0.1 mL), were inoculated *ip* parasitemia was scrutinized by microscopic examination of Giemsa stained smears (Dorn et al. 1995; Romero et al. 2018).

Four-day suppressive test

Caudal vein *iv* infection of Balb-C mice (18–23 g) was performed with 10^6 *P. berghei* infected red blood cells ($n = 6$). Two hours after infection, the active in vitro compounds (inhibition of β-hematin formation) were used for treatment. The active compounds were dissolved in DMSO (0.1 M), subsequently diluted with Saline-Tween 20 solution (2 %). Active compounds (dose 10 mg kg^{-1}) were administered *ip* for 4 days. At day four, parasite load was assessed by examining Giemsa stained smears. Chloroquine (10 mg kg^{-1}) was used as a positive control. The survival time of mice infected with *P. berghei* and treated with saline solution was used as base control. Results were expressed as percentage of parasitemia and survival curve was based upon days of mice survival treated with the compound over survival of mice infected but non-treated (Peters and Robinson 1999; Romero et al. 2018).

Cytotoxic activity

The human cell lines Jurkat, Clone E6-1, HL60 and normal lymphocytes were maintained in culture RPMI 1640 media supplemented with 10% FBS (Hyclone), 100unitsmL^{-1} penicillin/0.1 mgmL^{-1} streptomycin and 1 mM glutamine (Sigma-Aldrich). The cells were incubated in a humidified atmosphere, at 37 °C, containing 5% CO_2 in all the experiments. In the experimental assays, 3×10^5 cells per mL were seeded in 96 U well plates (Corning). All experimental assays were executed five times in triplicate (Romero et al. 2018).

Isolation of human totals lymphocytes

Heparinised blood was collected with written consent from healthy human volunteers as specified by the Ethical Committee at the Institute of Immunology. Peripheral blood mononuclear cells (PBMCs) were isolated by density gradient centrifugation using the standard Ficoll-Paque gradient (Histopaque 1077, Sigma, Poole, UK), for 30 min at 500x*g*. The obtained PBMC was washed twice with RPMI 1640 medium and cells obtained were resuspended in complete media and counted. Monocytes were depleted by cell adherence to plastic for 1 h at 37 °C. After monocyte depletion, cells were analyzed by flow cytometry. The resulting mononuclear cells were 85% T lymphocytes, 8% B lymphocytes, and 7% NK cells. In each of the assays with cell lines, normal lymphocytes were used as a reference. Each experiment was with a different donor. No differences were recorded among donors (Romero et al. 2018).

The 3-(4,5-Dimethyl-2-thiazolyl)-2,5-diphenyl-2H-tetrazolium bromide (MTT) viability assay

A slight modification of Mossman's MTT protocol (Mossmann 1983), described previously, (Suárez et al. 2009; Romero et al. 2018) was used to asses cell viability. Cells, 5×10^4 cells per well, were plated in 96-well microtiter plates in sextuplicate. The total volume was adjusted to 200 µL of complete culture medium containing 0, 1, 5, 10, 25, 50 and 100 µM concentrations of **3a, b, 4a–n,** and **5a–n** derivatives. Plates were incubated for 24 h, at 37 °C in a humidified incubator. At the end of the incubation, MTT (0.50 mgmL^{-1} in phosphate-buffered saline) was added to each well and further incubated for 4 h; then, centrifuged and washed with PBS to remove excess MTT. The formed formazan crystals were dissolved with DMSO and the plates were read using a microplate reader at 540 nm. The effect of compounds **3a, b, 4a–n**, and **5a–n** was reported as per cent cell viability using as controls cells incubated in complete media. The concentration of compound required to induce a 50% reduction of absorbance as compared to non-treated control was defined as IC_{50}. The positive controls of the assay were chloroquine, doxorubicin, and As_2O_3.

Annexin V/propidium iodide labeling

Both cell lines, Jurkat, Clone E6-1, HL60, were treated as aforementioned, then washed twice with PBS and

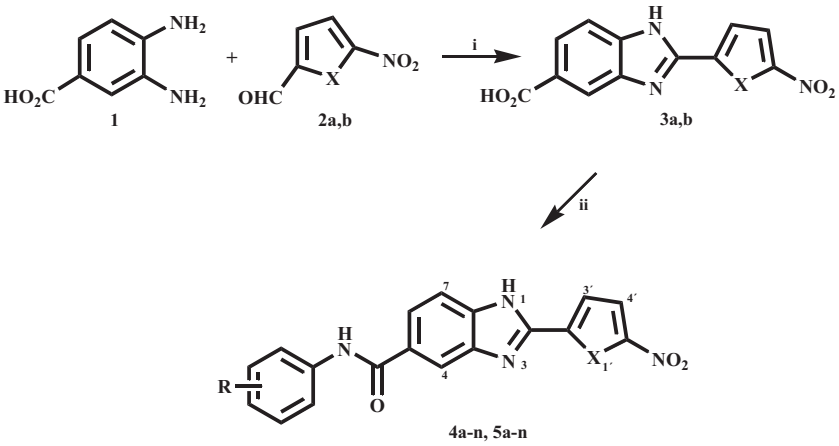

Fig. 1 Synthesis of N´-substituted-2-(5-nitrofuran or 5-nitrothiophen-2-yl)-3*H*-benzo[d]imidazole-5-carboxamide derivatives **4a–n**, **5a–n**.

i: nitrobenzene, Δ. **ii**: EDC, DMAP, DMF, 0 °C ⟶ rt,
X: O, S. **R**: H, OCH_3, CH_3, Cl, Br, CF_3

resuspended in Annexin V binding buffer (0.01 M HEPES, 0.14 M NaCl, and 2.5 mM $CaCl_2$). Annexin V-FITC conjugate (Santa Cruz Biotechnology) and propidium iodide (20 μgmL^{-1}) were added as recommended by the manufacturer. Analysis was performed using an Epics XL flow cytometer (Beckman Coulter). Untreated cells were used as negative controls and cells treated with quercetin (50 μM), chloroquine (100 μM), or doxorubicin (1 μM) were used as positive controls (Mijares et al. 2013; Romero et al. 2018).

A double plot analysis Annexin V-FITC (membrane apoptosis), propidium iodide (necrosis) was performed. The cells positive for both fluorochromes were defined as cells in late apoptosis, and cells negative to both fluorochromes as alive cells. As expected, positiveness was never higher than 2% in normal lymphocytes in non-treated cells and in treated cells with concentrations up to 5 μM. Doxorubicin, quercetin, and chloroquine were used as controls for apoptosis (Mijares et al. 2013). The concentration of doxorubicin was fixed at 1 μM as recommended in the literature (Mijares et al. 2013). Similarly, Baran et al. 2010; Chen et al. 2005; Wei et al. 1994; Santos et al. 2016 reported that 40–60 μM quercetin induced apoptosis in both cell lines. Martínez et al. 2010, showed an IC_{50} of 95 μM for chloroquine using the Jurkat E6.1 cell line. The concentrations of the drugs tested were not higher than 100 μM since DMSO may affect the results of the assay. Therefore, 1 μM doxorubicin, 50 μM quercetin, and 100 μM chloroquine were used as positive controls in both cell lines.

The IC_{50}values of the five most active derivatives were: 2.08 ± 0.10μM to 7.29 ± 0.86μM for HL60 cells, and 2.99 ± 0.24μM to 11.99 ± 0.98μM for Jurkat cells. Taking these values into account, the concentrations used for apoptosis assays were 1, 2.5, and 5μM. The highest concentration was represented in the final graphs of apoptosis in order to compare compound efficiency.

Data analysis

One-way analysis of variance and *t*-tests for specific group comparisons were used for data analysis. The program used was GraphPad Prism 3.02 (GraphPad Prism Software Inc. 1992–2004).

Results and discussion

Synthesis

Figure 1 illustrates a simple, straight forward strategy, used for the synthesis of compounds **4a–n** and **5a–n**. Compounds **3a**, **b** were obtained by the reaction of 3,4-Diaminobenzoic acid **1** with 5-Nitro-2-furaldehyde (**2a**) or 5-Nitro-2-thiophencarboxaldehyde (**2b**), using as solvent and oxidant nitrobenzene to obtain high yields of the described products (Charris et al. 2006). The corresponding amides **4a–n**, **5a–n** were obtained under a adapted version of the Steglich esterification reaction among carboxylic acid **3a–b** with the appropriately substituted aniline using EDC, DMAP in DMF, at room temperature, to generate the anticipated molecules (Neises and Steglich 1978). The final compounds were purified by recrystallization from ethanol-water, and the structure of the compounds was confirmed by IR, ^{1}H-NMR and elemental analysis. The IR spectra of compounds **4a–n** and **5a–n** showed broad stretching bands, around 3549 and 3580 cm^{-1} due to (NH), around 1650 and 1680cm^{-1} due to (CO), and around 1530–1510 cm^{-1} and 1350–1340 cm^{-1} due to (NO_2). In ^{1}H-NMR analysis, a singlet around 9.80 and 10.55ppm, doublets around 7.30 and 8.25ppm $J = 3$-4 Hz assigned to protons $H_{3'}$ and $H_{4'}$ respectively and benzimidazole moiety protons as doublets around 7.7ppm $J = 8.5$ Hz assigned to proton H_7, doublet

around 7.9ppm $J = 8.5$ Hz assigned to proton H_6, and doublets around 8.3ppm $J = 2.0$ Hz assigned to proton H_4. The structures of all obtained compounds were further supported by ^{13}C NMR spectra, one carboxyl groups of amide at chemical shift around 164 and 166ppm approximately was observed.

Biological

Antimalarial activity

Compounds generated were tested in vitro as inhibitors of β-H formation, and in vivo as antimalarial using a murine model (Table 1). The in vitro assay was used to evaluate the capabilities of the derivatives **4a–n**, **5a–n** to block β-H formation. Inhibition of heme crystallization was used as a standard assessment of antimalarial effect (Baelmans et al. 2000) and consequently, more than 80% of inhibition of heme crystallization was considered significant in our assays. With exception of compounds **3a** and **3b** with value of 76.45 ± 0.03 and 75.41 ± 0.003% respectively, the compounds **4d**, **4f**, **4l**, **5f**, and **5l**, Table 1, were considered effective. However, its activity was less than chloroquine (98.52 ± 0.01%).

In the structure/function analysis, the 5-Nitrofuril moiety appeared to be favorable for a potential antimalarial activity. Most of the compounds with this moiety were able to block β-H formation. Compounds **5f** and **5l** with 5-Nitrothiophene moiety also showed good activity despite not having the 5-Nitrofuril moiety. Structures with N-(Dimethylphenyl) carboxamide, and N-(4-Chlorophenyl) carboxamide groups in position five of benzimidazole exhibited very good activity. However, when in position two of benzimidazole there is a 5-Nitrofuril or a 5-Nitrothiophene moiety, and a mono, di, or tri substituted methoxy, or mono methyl, 2-chloro, 4-bromo or (trifluorophenyl) carboxamide groups a weak activity against inhibition of β-hematin formation was observed.

A chloroquine-susceptible strain of murine malaria *P. berghei* ANKA was used to infect mice. Infected mice were treated *ip* once daily for 4 consecutive days with 10 mg kg^{-1} of chloroquine (positive control) or **3a**, **3b**, **4d**, **4f**, **4l**, **5f**, and **5l** and after 4 days, parasitemia was evaluated. Survival of the treated mice was compared with control mice receiving a saline solution (untreated mice). Control mice died within 8.20 ± 0.20 days post-infection, compounds **3a** and **4d** increased survival rate to 17.00 ± 1.26, and 20.20 ± 1.95 days, respectively. Chloroquine prolonged mice survival rate to 29.20 ± 0.80 days. Compounds **3a** and **4d** were able to decrease and delay the progression of malaria (4.02 ± 0.45, and 3.05 ± 0.09 %), but did not eradicate infection as compared to chloroquine 0.80 ± 0.037 (Table 1).

The precise mechanism by which β-H inhibitors inhibit crystal growth is under dispute. For many years, it has been hypothesized that the inhibition recorded with quinoline antimalarials involve an interaction between the compound and Fe(III)PPIX. de Villiers et al. 2012, reported crystal structures of quinidine-heme (QD-Fe(III)PPIX) and quinine-heme (QN-Fe(III)PPIX) complexes, showing that there are three key interactions involved in heme binding by these particular drugs: coordination, hydrogen bonding, and π–π stacking. Recently, another study showed that some benzamides are capable of binding to Fe(III)PPIX through all three of these interactions: a pyridyl N for coordination, an amide for hydrogen bonding and aromatic rings for π–π stacking (Wicht et al. 2016).

Taking these studies into consideration, we propose that compounds (**4d**, **4f**, **4l**, **5f**, and **5l**) retain similar features. They are capable of bind to Fe(III)PPIX via all three of these interactions: a 5-Nitrofuril or 5-Nitrothiophene for coordination, an amide for hydrogen bonding and aromatic rings for π–π stacking. Although the particular requirements for π–π stacking are still unclear, we hypothesize that having larger planar aromatic molecular surfaces would enhance the strength of the interaction of the compounds with Fe(III)PPIX, to which we can also add the lipophilic influence of the N-(2, 4 or 3, 4-Dimethylphenyl) carboxamide, and N-(4-Chlorophenyl) carboxamide substituents, while the mono, di, or tri substituted methoxy, or mono methyl, 2-chloro, 4-bromo or (trifluoromethylphenyl) carboxamide groups were not tolerated. For compounds **3a** and **3b** the position 5 bears a carboxy group that could act as hydrogen bond acceptor.

Cytotoxic activity

MTT assay was use to analyze the effect of compounds **4a–n** and **5a–n** on cell viability in vitro against two cell lines. Freshly isolated human lymphocytes from normal donors were used as controls. Doxorubicin, chloroquine, and As_2O_3 were taken as positive controls and the IC_{50} values are summarized in Table 2. Compounds **3a**, **b**, **4d**, **f**, **g**, **i**, **k**, **l**, **m**, and **5b**, **d**, **e**, **i**, **k** showed very weak activity; compounds **4b**, **e**, **h**, **j**, and **5c**, **f**, **g**, **h**, **j**, **m** showed weak activity against the two human cancer cell lines. Compound **4c** exhibited moderate activity.

Compounds **4a**, **n** and **5a**, **n** revealed strong cytotoxic activity against both cell lines as compared to doxorubicin, chloroquine, and As_2O_3. Particularly, in human normal lymphocytes, compounds **4a** and **5n** were less toxic than doxorubicin (see Table 2). Doxorubicin, despite being an effective anticancer drug, is highly toxic on normal lymphocytes.

Apoptosis assay

Cell death pathways was studied by incubating the cell lines with compounds **4a**, **c**, **e**, **h**, **j**, **n,** and **5a**, **c**, **j**, **l**, **m**, **n** for 24

Table 1 Percentage of inhibition of β-hematin formation (%IβHF)

No.	R	% IβHF(± SD)[a]	%P^{b}(± SD)[a]	Sd[c](± SD)[a]	Survival[d]
3a	–	76.45 ± 0.03	4.02 ± 0.45**	17.00 ± 1.26**	0/6
3b	–	75.41 ± 0.003	11.5 ± 2.06	12.20 ± 1.15	0/6
4a	3,4,5-OCH_3	10.38 ± 0.16			
4b	2,4-OCH_3	74.24 ± 0.027			
4c	3-OCH_3	57.40 ± 0.13			
4d	2,4-CH_3	86.49 ± 0.044*	3.05 ± 0.09**	20.20 ± 1.95**	0/6
4e	2,5-CH_3	36.45 ± 0.088			
4f	3,4-CH_3	85.62 ± 0.066*	19.66 ± 1.76	8.80 ± 1.53	0/6
4g	3,5-CH_3	35.15 ± 0.04			
4h	3-CH_3	39.22 ± 0.027			
4i	2-CH_3	77.15 ± 0.053			
4j	3-Cl-4-OCH_3	67.27 ± 0.105			
4k	2-Cl	1.99 ± 0.009			
4l	4-Cl	88.74 ± 0.008*	47.00 ± 1.32	10.61 ± 1.14	0/6
4m	4-Br	76.96 ± 0.005			
4n	4-CF_3	5.19 ± 0.08			
5a	3,4,5-OCH_3	12.03 ± 0.037			
5b	2,4-OCH_3	20.43 ± 0.127			
5c	3-OCH_3	60.61 ± 0.079			
5d	2,4-CH_3	74.80 ± 0.04			
5e	2,5-CH_3	74.63 ± 0.04			
5f	3,4-CH_3	82.51 ± 0.001*	52.00 ± 0.36	8.80 ± 0.14	0/6
5g	3,5-CH_3	65.54 ± 0.044			
5h	3-CH_3	39.04 ± 0.015			
5i	2-CH_3	74.19 ± 0.116			
5j	3-Cl-4-OCH_3	20.43 ± 0.062			
5k	2-Cl	62.62 ± 0.0358			
5l	4-Cl	95.58 ± 0.081*	44.66 ± 0.69	10.20 ± 1.98	0/6
5m	4-Br	21.07 ± 0.178			
5n	4-CF_3	12.82 ± 0.286			
CQ	–	98.52 ± 0.01	0.80 ± 0.037	29.20 ± 0.80	5/6
CiSS	–	–	61.33 ± 1.40	8.20 ± 0.20	0/6

Effect of derivatives **3a–b**, **4a–n**, and **5a–n** on *P. berghei* infected mice infection (10 $mgkg^{-1}$)

X: **3a**, (**5a–n**) = **O**; X: **3b** (**5a–n**) = **S**

CQ chloroquine, *CiSS* control infected and treated with saline solution

*$p > 0.05$ compared to chloroquine. **$p < 0.001$ compared to saline solution and chloroquine. $n = 6$

[a]SD: Standard deviation

[b]%P: Percentage of parasitemias

[c]Sd: Survival days

[d]Number of mice that survived till day 30 post-infection/total mice in the group

h. Apoptosis and necrosis were analyzed by flow cytometry using Annexin V-FITC and propidium iodide (Choi et al. 2008). Doxorubicin, chloroquine, and quercetin were taken as controls due to its anti-leukemic effect (Wei et al. 1994; Chen et al. 2005; Baran et al. 2010; Mijares et al. 2013; Maso et al. 2014; Li et al. 2016). The Fig. 2a, b, illustrates a typical flow cytometry assay for apoptosis and necrosis. Early and late apoptosis are clearly observed upon treatment and necrosis is very low in all the conditions tested.

The main alterations recorded are the increase in Annexin V-FITC positiveness (early apoptosis). Propidium iodide positiveness was only recorded in late apoptosis and not as simple necrosis. The results are summarized in Table 3 and 4 (Supplementary Materials).

Table 2 Effect of derivatives **3a**, **b**, **4a–n**, and **5a–n**, 1 → 100(μM), on cell viability assessed by the MTT method

No.	R	Normal lymphocytes	Jurkat E6.1 IC_{50}(± SD) 24 h	HL60 IC_{50} (± SD) 24 h	Selectivity index Jurkat E6.1	Selectivity index HL60
3a	-	ND	>100	>100		
3b	-	ND	>100	>100		
4a	3,4,5-OCH_3	55.29 ± 6.21	7.05 ± 0.60*	2.95 ± 0.28*	7.84	18.74
4b	2,4-OCH_3	ND	46.26 ± 3.54	20.82 ± 2.94		
4c	3- OCH_3	83.55 ± 6.25	12.11 ± 1.69	7.35 ± 0.56	6.90	11.36
4d	2,4-CH_3	ND	>100	>100		
4e	2,5-CH_3	51.06 ± 3.66	41.53 ± 4.35	26.74 ± 4.11	6.16	1.91
4f	3,4-CH_3	ND	>100	75.11 ± 5.66		
4g	3,5-CH_3	ND	>100	>100		
4h	3-CH_3	86.63 ± 8.90	20.78 ± 1.99	8.59 ± 0.93	3.36	10.08
4i	2-CH_3	ND	>100	>100		
4j	3-Cl-4-OCH_3	79.34 ± 3.60	26.39 ± 2.05	11.15 ± 0.59	3.01	7.11
4k	2-Cl	ND	>100	>100		
4l	4-Cl	ND	>100	>100		
4m	4-Br	ND	>100	>100		
4n	4-CF_3	57.99 ± 5.24	10.79 ± 1.25*	4.29 ± 0.69*	5.37	13.52
5a	3,4,5-OCH_3	64.18 ± 4.89	11.88 ± 1.21*	6.64 ± 0.67*	5.40	9.67
5b	2,4-OCH_3	ND	>100	>100		
5c	3- OCH_3	>100	44.00 ± 2.39	18.05 ± 2.74	>2.27	>5.54
5d	2,4-CH_3	ND	>100	>100		
5e	2,5-CH_3	ND	>100	>100		
5f	3,4-CH_3	ND	81l.32 ± 9.06	38.99 ± 4.53		
5g	3,5-CH_3	ND	53.97 ± 7.63	28.39 ± 2.59		
5h	3-CH_3	ND	67.49 ± 6.62	33.16 ± 2.97		
5i	2-CH_3	ND	>100	>100		
5j	3-Cl-4-OCH_3	>100	21.86 ± 3.52	9.38 ± 1.05	>4.57	>10.66
5k	2-Cl	ND	>100	>100		
5l	4-Cl	75.01 ± 8.56	12.08 ± 1.04	7.50 ± 0.28	6.21	10.0
5m	4-Br	87.16 ± 9.41	23.60 ± 3.42	18.5 ± 1.46	3.69	4.71
5n	4-CF_3	67.78 ± 6.94	12.12 ± 1.16*	3.68 ± 0.43*	5.59	18.42
CQ	--	>100	80.35 ± 9.65	94.63 ± 5.60	>1.24	>1.06
Dox	--	4.36 ± 0.30	1.49 ± 0.13	2.48 ± 0.27	2.92	1.76
As_2O_3	--	15.27 ± 1.34	8.86 ± 0.26	6.04 ± 0.85	1.72	2.53

Selectivity index cytotoxicity relative to normal lymphocytes. Results are expressed as the mean IC_{50} of three experiments. IC_{50} was calculated by non-linear regression (variable slope) analysis using GraphPad Prism

SD standard deviation, *Jurkat E6.1* acute lymphocytic leukemia, *HL60* acute myelogenous leukemia, *CQ* chloroquine, *Dox* doxorubicin, *ND* not determined

*$p < 0.01$ compared to doxorubicin.

The induction of Annexin V-FITC positiveness upon treatment was different in each cell line. After 24 h, in the HL60 cell line, the maximum apoptosis was recorded using 10 μM. Annexin V-FITC expression was 50% or higher in cells treated with 10μM of compounds **4a**, **c**, **h**, **n**, **5a**, **l,** and **n**. Compound **4j** was less effective, <50%. Conversely, there was no significant increase in the Annexin V-FITC fluorescence when Jurkat cells were treated with those compounds. The exception was compound **4a**, which was very active at 10 μM. Doxorubicin, positive control, was highly effective at 1 μM. The tested structures did not produce necrosis as can be seen in Fig. 2a, b. The effects of the compounds on apoptosis and necrosis are illustrated in Table 3.

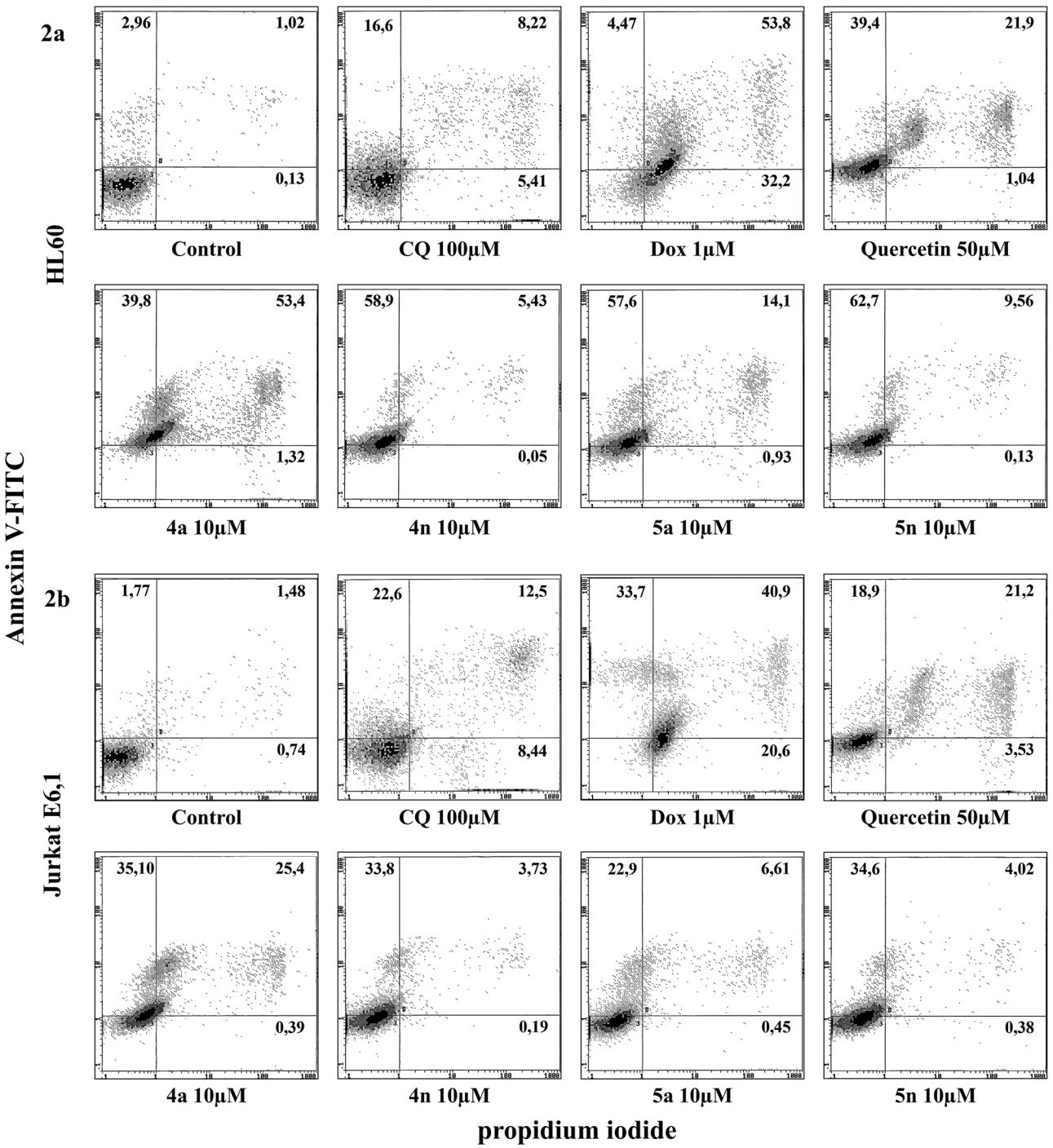

Fig. 2 **a**, **b** Apoptosis effect on human HL60 and Jurkat E6.1 cells induced by compounds **4a**, **4n**, **5a**, and **5n**. Apoptosis cells were detected with Annexin V-FITC/PI double staining after incubation with compounds **4a**, **4n**, **5a**, and **5n** (10 µM), CQ (100 µM), Dox. (1 µM), Querc. (50 µM), or control for 24 h. Percentages of cells in each quadrant are given as non-apoptotic live (lower left), necrotic dead (lower right), early apoptotic (upper left), and late apoptotic (upper right). A representative experiment is shown

The structure–activity relationship seems to differ among the two models studied. The effect of electron deficient versus electron rich aromatic rings (phenylcarboxamide) on those compounds like the OCH_3 groups in positions 3, 4, 5 and a group 5-Nitrofuril in position 2 of benzimidazol are better tolerated, while strongly attractor groups of electrons in position 4 like Cl, Br, or CF_3 added to a group 5-Nitrothiophene in the position 2 of the benzimidazol favor the anticancer activity but to a lesser extent than the electron donator groups.

Conclusion

The compounds were assessed in vitro as potential blockers of β-hematin formation, only five (**4d**, **4f**, **4l**, **5f**, and **5l**) showed a significant inhibition value (% IβHF > 80). The benzimidazole derivatives (**3a**, **3b**, **4d**, **4f**, **4l**, **5f**, and **5l**) were then chosen and analyzed in mice infected with *P. berghei* ANKA chloroquine-susceptible strain. Compounds **3a** and **4d** exhibited important antimalarial activity comparable to that of chloroquine. Cytotoxic activity against two human cancer cell lines and human normal lymphocytes was used to screen the different structures. An extraordinary in vitro anticancer activity was observed in structure **4a**, comparable to doxorubicin. Counter wise, compound **4a** does not affect human normal leukocytes viability at 10 μM. This excellent activity/toxicity profile has to be tested in several other cancer models.

Data from flow cytometry studies confirmed that compound **4a** inhibits proliferation of HL60, and Jurkat E6.1 cancer cells and promotes apoptosis. The mechanism of action of compound **4a** could be related to the inhibition of heme synthesis or the inhibition of lysosome induced autophagy (Zhang et al. 2013; Manic et al. 2014; Li et al. 2016).

A preliminary analysis of the structure–activity relationships (SAR) of the compounds evaluated in this study leads us to propose that the benzimidazole-5-carboxamide derivatives with the subsequent structural characteristics are preferred to display significant antiplasmodial activity. The characteristics are: (a) the presence of benzimidazole unit may involve π–π stacking interaction with the porphyrin ring system, (b) a 5-nitrofuran-2-yl or a 5-nitrothyophen-2-yl on the 2-position of the benzimidazole ring unit, and (c) the presence of a phenylcarboxamide in position 5 with a replacement pattern of 2, 4 or 3, 4 with lipophilic groups. On the other hand, the anticancer activity was found to be more pronounced in compounds with: (d) the presence of a 5-nitrofuran-2-yl on the 2-position of the benzimidazole ring unit, and (e) the presence of a phenylcarboxamide in position 5 with methoxy groups on 3,4,5; monosubstituted with trifluoromethyl group on the 4-position.

The comprehensive relationship between antiparasitic activity, inhibition of hemozoin formation, and anticancer activity for this type of compound has been observed. Therefore, a potent inhibition of heme formation does not guarantee the antimalarial or anticancer activities. These results provide an understanding of the structural features that influence functional activity for this class of compounds and also offer new possibilities for improvements in the antimalarial and anticancer performances of benzimidazole-5-carboxamide derivatives. Further studies shall determine the importance of this different structures.

Acknowledgements We thank the IIF and CDCH-UCV (grants IIF.02-2017, PG. 06-8627-2013/2) programs for financial support.

Compliance with ethical standards

Conflict of interest The authors declare that they have no conflict of interest.

References

Akhtar W, Khan M, Verma G, Shaquiquzzaman M, Rizvi M, Mehdi S, Akhter M, Alam M (2017) Therapeutic evolution of benzimidazole derivatives in the last quinquennial period. Eur J Med Chem 126:705–753

Baelmans R, Deharo E, Muñoz V, Sauvain M, Ginsburg H (2000) Experimental conditions for testing the inhibitory activity of chloroquine on the formation of β-hematin. Exp Parasitol 96:243–248

Bansal Y, Silakari O (2012) The therapeutic journey of benzimidazoles: A review. Bioorg Med Chem 20:6208–6236

Baran I, Ganea C, Scordino A, Musumeci F, Barresi V, Tudisco S, Privitera S, Grasso R, Condorelli D, Ursu I, Baran V, Katona E, Mocanu M-M, Gulino M, Ungureanu R, Surcel M, Ursaciuc C (2010) Effects of menadione, hydrogen peroxide, and quercetin on apoptosis and delayed luminescence of human leukemia Jurkat T-cells. Cell Biochem Biophys 58:169–179

Berger T, Dieckmann D, Efferth T, Schultz E, Funk J, Baur A, Schuler G (2005) Artesunate in the treatment of metastatic uveal melanoma-first experiences. Oncol Rep 14:1599–1603

Brain-Isasi S, Quezada C, Pessoa H, Morello A, Kogan M, Alvarez-Lueje A (2008) Determination and characterization of new benzimidazoles with activity against Trypanosoma cruzi by UV spectroscopy and HPLC. Bioorg Med Chem 16:7622–7630

Camacho J, Barazarte A, Gamboa N, Rodrigues J, Rojas R, Vaisberg A, Gilman R, Charris J (2011) Synthesis and biological evaluation of benzimidazole-5-carbohydrazide derivatives as antimalarial, cytotoxic and antitubercular agents. Bioorg Med Chem 19:2023–2029

Charris J, Camacho J, Ferrer R, Lobo G, Barazarte A, Gamboa N, Rodrigues J, López S (2006) A convenient route to 2-substituted benzothiazole-6-carboxylic acids using nitrobenzene as oxidant. J Chem Res 12:769–770

Charris J, Lobo G, Camacho J, Ferrer R, Barazarte A, Domínguez J, Gamboa N, Rodrigues J, Ángel J (2007) Synthesis and antimalarial activity of (E) 2-(2´-Chloro-3´-quinolinylmethylidene)-5,7-dimethoxyindanones. Lett Drug Des Dis 4:49–54

Chen D, Daniel K, Chen M, Kuhn D, Landis-Piwowar K, Dou Q (2005) Dietary flavonoids as proteasome inhibitors and apoptosis inducers in human leukemia cells. Biochem Pharmacol 69:1421–1432

Chloroquine Phosphate Oral, 21 may 2018. http://nlm.nih.gov/medlineplus/druginfo/meds/a682318.html. Accessed 20 June 2018

Cho Y, Ioerger T, Sacchettini J (2008) Discovery of novel nitrobenzothiazole inhibitors for Mycobacterium tuberculosis ATP phosphoribosyl transferase (HisG) through virtual screening. J Med Chem 51:5984–5992

Choi E, Bae S, Ahn W (2008) Antiproliferative effects of quercetin through cell cycle arrest and apoptosis in human breast cancer MDA-MB-453 cells. Arch Pharm Res 31:1281–1285

de Villiers K, Gildenhuys J, Roex T (2012) Iron(III) protoporphyrin IX complexes of the antimalarial cinchona alkaloids quinine and quinidine. ACS Chem Biol 7:666–671

Dondorp A, Nosten F, Yi P, Das D, Phyo A, Tarning J, Lwin K, Ariey F, Hanpithakpong W, Lee S, Ringwald P, Silamut K, Imwong M, Chotivanich K, Lim P, Herdman T, An S, Yeung S, Singhasivanon P, Day N, Lindegardh N, Socheat D, White N (2009) Artemisinin resistance in Plasmodium falciparum malaria. N Engl J Med 361:455–467

Dorn A, Stoffel R, Matile H, Bubendorf A, Ridley R (1995) Malarial haemozoin/beta-haematin supports haem polymerization in the absence of protein. Nat (Lond) 374:269–271

Efferth T, Sauerbrey A, Olbrich A, Gebhart E, Rauch P, Weber H, Hengstler J, Halatsch M, Volm M, Tew K, Ross D, Funk J (2003) Molecular modes of action of artesunate in tumor cell lines. Mol Pharmacol 6:382–394

Efferth T (2007) Willmar Schwabe Award 2006: antiplasmodial and antitumor activity of artemisinin-from bench to bedside. Planta Med 73:299–309

Egan T, Ncokazi K (2005) Quinoline antimalarials decrease the rate of β-hematin formation. J Inorg Biochem 99:1532–1539

Gaba M, Mohan C (2016) Development of drugs based on imidazole and benzimidazole bioactive heterocycles: recent advances and future directions. Med Chem Res 25:173–210

Gaba M, Singh S, Mohan C (2014) Benzimidazole: An emerging scaffold for analgesic and anti-inflammatory agents. Eur J Med Chem 76:494–505

Graph Pad Prism Software Inc. 4.02 for windows. May 17th. La Jolla, CA, 92037 USA (1992–2004)

Gupta S, Sung B, Prasad S, Webb L, Aggarwal B (2013) Cancer drug discovery by repurposing: teaching new tricks to old dogs. Trends Pharmacol Sci 34:508–517

Handrick R, Ontikatze T, Bauer K, Freier F, Rübel A, Dürig J, Belka C, Jendrossek V (2010) Dihydroartemisinin induces apoptosis by a bak-dependent intrinsic pathway. Mol Cancer Ther 9:2497–2510

Hooft van Huijsduijnen R, Guy R, Chibale K, Haynes R, Peitz I, Kelter G, Phillips M, Vennerstrom J, Yuthavong Y, Wells T (2013) Anticancer properties of distinct antimalarial drug classes. PLoS ONE 8:e82962

Hosseinzadeh N, Hasani M, Foroumadi A, Nadri H, Emami S, Samadi N, Faramarzi M, Saniee P, Siavoshi F, Abadian N, Mahmoudjanlou Y, Sakhteman A, Moradi A, Shafiee A (2013) 5-Nitroheteroarylidene analogs of 2-thiazolylimino-4-thiazolidinones as a novel series of antibacterial agents. Med Chem Res 22:2293–2302

Joshi A, Viswanathan C (2006) Recent developments in antimalarial drug discovery. Anti-Infec Agents Med Chem 5:105–122

Kangwan N, Park J, Kim E, Hahm K (2014) Chemoquiesence for ideal cancer treatment and prevention: where are we now? J Cancer Prev 19:89–96

Kim P, Kang S, Boshoff H, Jiricek J, Collins M, Singh R, Manjunatha U, Niyomrattanakit P, Zhang L, Goodwin M, Dick T, Keller T, Dowd C, Barry C (2009) Structure-activity relationships of antitubercular nitroimidazoles. 2. Determinants of aerobic activity and quantitative structure-activity relationships. J Med Chem 52:1329–1344

Kim E, Stenberg R, Ru bsam A, Schmitz-Salue C, Warnecke G, Bücker E, Pettkus N, Speidel D, Rohde V, Schulz-Schaeffer W, Deppert W, Giese A (2010) Chloroquine activates the p53 pathway and induces apoptosis in humanglioma cells. Neuro-Oncol 12:389–400

Kundu C, Das S, Nayak A, Satapathy S, Das D, Siddharth S (2015) Anti-malarials are anti-cancers and vice versa – One arrow two sparrows. Acta Trop1 49:113–127

Lai H, Singh N (2006) Oral artemisinin prevents and delays the development of 7,12 dimethylbenz[a]anthracene (DMBA)-induced breast cancer in the rat. Cancer Lett 231:43–48

Lan P, Romero F, Wodka D, Kassick A, Dang Q, Gibson T, Cashion D, Zhou G, Chen Y, Zhang X, Zhang A, Li Y, Trujillo M, Shao Q, Wu M, Xu S, He H, MacKenna D, Staunton J, Chapman K, Weber A, Sebhat I, Makara G (2017) Hit-to-lead optimization and discovery of 5-((5-([1,1'-Biphenyl]-4-yl)-6-chloro-1H-benzo[d]imidazol-2-yl)oxy)-2-methylbenzoic acid (MK-3903): A novel class of benzimidazole based activators of AMP-activated protein kinase. J Med Chem 60:9040–9052

Li Y, Zeng X, Wang S, Fan J, Wang Z, Song P, Mei X, Ju D (2016) Blocking autophagy enhanced leukemia cell death induced by recombinant human arginase. Tumour Biol 37:6627–6635

Manic G, Obrist F, Kroemer G, Vitale L, Galluzzi L (2014) Chloroquine and hydroxychloroquine for cancer therapy. Mol Cell Oncol 1:e29911

Martínez A, Rajapakse C, Sánchez-Delgado R, Varela-Ramírez A, Lema C, Aguilera R (2010) Arene-Ru(II)-chloroquine complexes interact with DNA, induce apoptosis on human lymphoid cell lines and display low toxicity to normal mammalian cells. J Inorg Biochem 104:967–977

Maso V, Calgarotto A, Franchi Jr G, Nowill A, Filho P, Vassallo J, Olalla S (2014) Multitarget effects of quercetin in leukemia. Cancer Prev Res (Phila) 12:1240–1250

Meshnick S, Thomas A, Ranz A, Xu C, Pan H (1991) Artemisinin (qinghaosu): the role of intracellular hemin in its mechanism of antimalarial action. Mol Biochem Parasitol 49:181–189

Mijares M, Ochoa M, Barroeta A, Martínez G, Suárez A, Compagnone R, Chirinos P, Avila R, De Sanctis J (2013) Cytotoxic effets of fisturalin-3 and 11-deoxyfisturalin-3 on jurkat and U937 cell lines. Biomed Pap 157:222–226

Mital A (2009) Synthetic nitroimidazoles: Biological activities and mutagenicity relationships. Sci Pharm 77:497–520

Mosmann T (1983) Rapid colorimetric assay for cellular growth and survival: application to proliferation and cytotoxicity assays. J Immunol Methods 65:55–63

Mushtaque S (2015) Reemergence of chloroquine (CQ) analogs as multi-targeting antimalarial agents: a review. Eur J Med Chem 90:280–295

Neises B, Steglich W (1978) Simple method for the esterification of carboxylic acids. Angew Chem Int Ed Engl 17:522–524

Njaria P, Okombo J, Njuguna N, Chibale K (2015) Chloroquine-containing compounds: a patent review (2010-2014). Expert Opin Ther Pat 25:1003–1024

Noedl H, Se Y, Schaecher K, Smith B, Socheat D, Fukuda M (2008) Evidence of artemisinin-resistant malaria in western Cambodia. N Engl J Med 359:2619–2620

Noedl H, Socheat D, Satimai W (2009) Artemisinin-resistant malaria in Asia. N Engl J Med 361:540–541

Nordstrøm L, Sironi J, Aranda E, Maisonet J, Perez-Soler R, Wu P, Schwartz E (2015) Discovery of autophagy inhibitors with antiproliferative activity in lung and pancreatic cancer cells. ACS Med Chem Lett 6:134–139

O'Neill P, Barton V, Ward S (2010) The molecular mechanism of action of artemisinin-the debate continues. Molecules 15:1705–1721

Peters W, Robinson B (1999) Parasitic infection models. In: Zak O, Sande M (eds) Handbook of antimalarial models of infection. Academic Press, London, p 757

Phillips M, Burrows J, Manyando C, van Huijsduijnen R, van Voorhis W, Wells T (2017) Malaria. Nat Rev Dis Prim 3:17050

Posner G, McRiner A, Paik I, Sur S, Borstnik K, Xie S, Shapiro T, Alagbala A, Foster B (2004) Anticancer and antimalarial efficacy and safety of artemisinin-derived trioxane dimers in rodents. J Med Chem 47:1299–1301

Rodrigues J, Charris J, Ferrer R, Gamboa N, Ángel J, Nitzsche B, Hoepfner M, Lein M, Jung K, Abramjuk C (2012) Effect of

quinolinyl acrylate derivatives on prostate cancer in vitro and in vivo. Invest New Drugs 30:1426–1433
Romero J, Acosta M, Gamboa N, Mijares M, De Sanctis J, Charris J (2018) Optimization of antimalarial, and anticancer activities of (E)-methyl 2-(7-chloroquinolin-4-ylthio)-3-(4-hydroxyphenyl) acrylate. Bioorg Med Chem 26:815–823
Santos G, Almeida M, Antunes L, Bianchi M (2016) Effect of bixin on DNA damage and cell death induced by doxorubicin in HL60 cell line. Hum Exp Toxicol 35:1319–1327
Singh B, Kim Sung L, Matusop A, Radhakrishnan A, Shamsul S, Cox-Singh J, Thomas A, Conway D (2004) A large focus of naturally acquired Plasmodium knowlesi infections in human beings. Lancet 363:1017–1024
Singh N, Panwar V (2006) Case report of a pituitary macroadenoma treated with artemether. Integr Cancer Ther 5:391–394
Siriram D, Yogeeswari P, Dhakla P, Senthilkumar P, Banerjee D, Manjashetty T (2009) 5-Nitrofuran-2-yl derivatives: Synthesis and inhibitory activities against growing and dormant mycobacterium species. Bioorg Med Chem Lett 19:1152–1154
Siriram D, Yogeeswari P, Kumar D, Senthilkumar P, Bhat P, Srividya M (2010) 5-Nitro-2-furoic acid hydrazones: Design, synthesis and in vitro antimycobacterial evaluation against log and starved phase cultures. Bioorg Med Chem Lett 20:4313–4316
Suárez A, Chávez K, Mateu E, Compagnone R, Muñoz A, Sojo F, Arvelo F, Mijares M, De Sanctis J (2009) Cytotoxic activity of seco-entkaurenes from Croton caracasana on human cancer cell lines. Nat Prod Commun 4:1547–1550
US Centers for Disease Control and Prevention. Atlanta, GA: CDC; (2016) http://www.cdc.gov/malaria/history/index.htm. (Accessed 02. 19. 2018)
Van Huijsduijnen R, Guy R, Chibale K, Haynes R, Peitz I, Kelter G, Phillips M, Vennerstrom J, Yuthavong Y, Wells T (2013) Anticancer properties of distinct antimalarial drug classes. PLoS ONE 8:e82962
Wei Y, Zhao X, Kariya Y, Fukata H, Teshigawara K, Uchida A (1994) Induction of apoptosis by quercetin: involvement of heat shock protein. Cancer Res 54:4952–4957
Wicht K, Combrinck J, Smith P, Hunter R, Egan T (2016) Identification and SAR evaluation of hemozoin-inhibiting benzamides active against Plasmodium falciparum. J Med Chem 59:6512–6530
World Health Organization, Media centre Cancer february (2018a) http://www.who.int/mediacentre/factsheets/fs094/en/. (Accessed 02.05.2018)
World Health Organization, Media centre Cancer february (2018b) http://www.who.int/mediacentre/factsheets/fs297/en/.(Accessed 02.05.2018)
World Health Organization, welcomes global health funding for malaria vaccine (2016)http://www.who.int/mediacentre/news/releases/2016/malaria-control-africa/en/. (Accessed 02. 19. 2018)
Xu Q, Li Z, Peng H, Sun Z, Cheng R, Ye Z, Li W (2011) Artesunate inhibits growth and induces apoptosis in human osteosarcoma HOS cell line in vitro and in vivo. J Zhejiang Univ Sci B 12:247–255
Yadav G, Ganguly S (2015) Structure activity relationship (SAR) study of benzimidazole scaffold for different biological activities: A mini-review. Eur J Med Chem 97:419–443
Zeng Q, Zhang P (2011) Artesunate mitigates proliferation of tumor cells by alkylating heme-harboring nitric oxide synthase. Nitric Oxide 24:110–112
Zhang S, Chen H, Webster J, Gerhard G (2013) Targeting heme for the identification of cytotoxic agents. Anti-Cancer Agents Med Chem 13:515–522
Zhang S, Gerhard G (2009) Heme mediates cytotoxicity from artemisinin and serves as a general anti-proliferation target. PLoS ONE 4:e7472
Zhou C, Pan W, Wang X, Chen T (2012) Artesunate induces apoptosis via a Bak-mediated caspase-independent intrinsic pathway in human lung adenocarcinoma cells. J Cell Physiol 227:3778–3786